COOLING RATES OF TYPE I CHONDRULES FROM THE RENAZZO CR2 CHONDRITE: IMPLICATIONS FOR CHONDRULE FORMATION. N. Chaumard[1], M. Humayun[2], B. Zanda[1], and R. H. Hewins[1,3], [1]IMPMC, MNHN, UPMC Université Paris 06, UMR CNRS 7590, IRD UMR 206, CP 52, 57 rue Cuvier, 75231 Paris Cedex 05, France (nchaumard@mnhn.fr), [2]Department of Earth, Ocean, and Atmospheric Science & National High Magnetic Field Laboratory, Florida State University, 1800 E. Paul Dirac Drive, Tallahassee, FL 32310, USA, [3]Department of Earth and Planetary Sciences, Rutgers University, Piscataway, NJ 08854, USA.

Introduction: Chondrules are ubiquitous components of carbonaceous chondrites (CCs) [e.g., 1]. Since the recognition of the igneous texture of chondrules by [2], numerous heating mechanisms have been proposed for chondrule formation, which were extensively commented and reviewed [e.g., 3].

The most evolved models involve either the Sun to explain the melting event at the origin of the chondrule formation, i.e., the X-wind model [e.g., 4], or high-temperature events that took place in the nebular gas. The latter include the lightning models [e.g., 5], planetesimal bow shocks [e.g., 6], and shock fronts possibly driven by gravitational instabilities and passing through the gas [e.g., 7,8]. These shock models were developed for the melting and evaporation of particles by shock waves in the protoplanetary disk, and they reproduce the cooling rates of 10–1000°C.h^{-1} experimentally estimated for chondrules [e.g., 9,10]. Alternative models, such as the collisions of partially melted planetesimals generating melt droplets have also been proposed [e.g., 11], but such models have not been extensively developed yet.

However, the mechanisms presented above were suggested on the basis of cooling rates estimated for Type II (oxidized) chondrules while CCs are dominated by Type I (reduced) chondrules. Only a few measurements of the cooling rates of Type I chondrules have been made so far, either based on pyroxene exsolution [12,13] or zoning profiles in metal grains [14,15]. We present here additional measurements of cooling rates of Type I chondrules that would provide useful constraints on chondrule formation. Since Fe-Ni metal is abundant in CR chondrites, we decided to use the method developed by [14] based on Cu and Ga zoning profiles measured by LA-ICP-MS, in metal associated with POP Type I chondrules in the Renazzo CR2 chondrite.

Methods: We imaged by CT scanning two fragments of Renazzo using a v|tome|x 240L from GE Sensing & Inspection Technologies Phoenix X|Ray in order to determine the center of metal grains. The cooling rates estimated are thus free from possible under-estimation due to the random sectioning. Therefore, we used X-ray tomography to locate Type I chondrules with large metal grains. Then, we cut our samples close to the equatorial planes of these selected metal grains and polished our sections until equatorial planes of these metal grains were exposed at the polished surface of our samples.

Laser ablation ICP-MS analyses were performed at Florida State University using a New Wave UP193 FX excimer laser ablation system coupled to a Thermo Element XR ICP-MS following the methods of [14,15]. Eight laser tracks were measured through the center of four (250–500 μm large) metal grains either included (B1) or attached (A1, A2, and C1) to 3 chondrules, using a 15 μm spot size, 5 μm.s^{-1} speed, 50 Hz repetition rate, 100% power output (1.55 GW.cm^{-2}). Each diffusion profile is characterized by a diffusion length-scale determined by numerically fitting an error function to the measured profiles using MatLab.

Results: All profiles measured display a chemical zonation in Cu and Ga. The border of metal grains is enriched in Cu and Ga while cores are depleted in these volatile siderophile elements relative to the edges. Maximum Cu and Ga contents at the borders range from 25 to 107 and from 1.8 to 5.4 ppm, respectively (Table 1). The cores of the metal grains contain a minimum of around 8 and 0.8 ppm of Cu and Ga, respectively. The U-shaped profiles have diffusion length-scales between 42 and 261 μm (Table 1).

Chondrule		A				B	C		
Metal grain		A1		A2		B1	C1		
Profile		36-A1	34-A1	41-A2	40-A2	23-B1	39-2C1	40-2C1	41-2C1
Diff. length-scale (μm)		121	59	42	109	261	91	69	50
Cu (ppm)	Max.	77	107	33	77	37	45	72	25
	Min.	12	19	14	14	13	9	10	8
Ga (ppm)	Max.	5.2	4.0	3.2	5.4	1.8	2.9	3.7	2.0
	Min.	0.8	1.6	1.1	2.1	0.9	0.9	1.3	1.0
	T_p (K)	1625	1625	1650	1700	1550	1725	1625	1650
	dT/dt (K.h^{-1})	9.3	39.1	96.7	23.3	0.9	41.2	29.3	68.7

Table 1: Diffusion length-scales, maximum and minimum abundances measured for Cu and Ga, and T_p and associated cooling rates for each diffusion profile measured.

Using the method of [14] based on the mutual diffusivities of Cu and Ga [16], we are able to provide an estimation of the temperature at which zoning profiles measured here were formed (T_p). Fig. 1 shows that our data largely overlap the 1644 K curve and globally plot between the 1473 and 1773 K curves. The values of T_p and the cooling rates associated for the 8 diffusion

profiles are reported in Table 1. All peak temperatures (1550–1725 K) and cooling rates (0.9–96.7 K.h^{-1}) estimated here are consistent from one metal grain to another for a single chondrule.

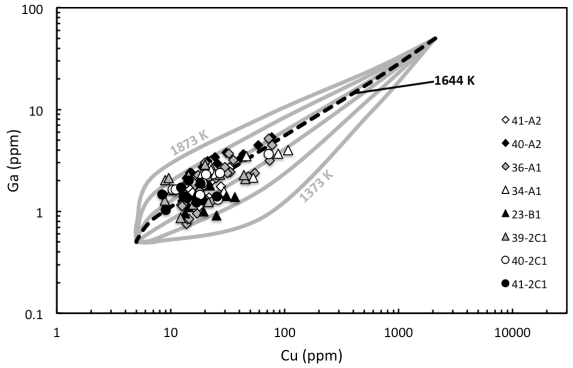

Fig. 1: Ga vs. Cu for the 8 profiles measured in Renazzo, as a function of temperature from 1873 to 1373 K in 100 K increments. Since the Ga contents in the cores of metal grains are close to the detection limit (~0.7 ppm), we only plotted points situated in the external parts of the diffusion profiles.

Discussion: The ubiquity of U-shaped profiles for Cu and Ga, even in metal grains situated within the chondrule B, indicates that large metal grains reacted with the ambient gas (evaporation and re-condensation of volatile siderophile elements). Considering that metal in CR chondrites originated from chondrules [e.g., 17,18], our data suggest that large metal grains were previously isolated from the liquid silicate as immiscible liquids then re-accreted within chondrules after reacting with the surrounding gas. These results also support a formation of chondrules in Renazzo by aggregation of droplets, as advocated by [18].

The homogeneity of the cooling rates estimated here and their consistency with those obtained by [14] (0.5–50 K.h^{-1} for T_p ~1473 K) for chondrules in the Acfer 097 CR2 chondrite, support a common origin of Type I chondrules in CR chondrites. Although globally lower than cooling rates experimentally determined for Type I chondrules (10–1000 K.h^{-1}; [3, and references therein]), these analytical results are not in conflict with these data since chondrule textures were formed at higher temperatures than the diffusion profiles measured here. Further, these results, which are also in good agreement with those obtained from pyroxene exsolution in Type I chondrules (2–10 K.h^{-1} for T_p ~1473–1623 K in Allende [12] and 10–100 K.h^{-1} in Paris [13]), support a similar solid-state thermal history and a common high-temperature event at the origin of the formation of Type I chondrules in CCs.

Fig. 2 shows that cooling rates are lower at lower peak temperatures, indicative of a more complex cooling curve than linear cooling curves used in experimental studies [e.g., 9,10]. These results are clearly at variance with the fast cooling rates predicted by the lightning models [e.g., 5], and to a lesser extent by the X-wind model [e.g., 4] even if the latter appears to be able to produce only low cooling rates (~<100 K.h^{-1}). The most relevant models for the formation of Type I chondrules in CCs are those invoking shock waves [e.g., 7,8].

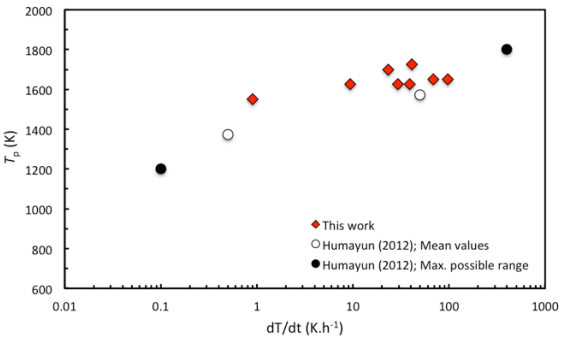

Fig. 2: Peak temperatures vs. cooling rates calculated from the 8 diffusion profiles of Cu measured in this work.

Conclusion: The plausible nonlinear cooling curves and cooling rates ranging from 0.9 to 96.7 K.h^{-1} are consistent with the predictions of shock wave models (10–300 K.h^{-1}) [e.g., 7,8]. This high temperature event appears to be the most feasible heating mechanism for the formation of Type I chondrules in CCs.

Acknowledgements: We thank the AST-RX computed tomography facility (UMS 2700 CNRS-MNHN, Paris) for CT-scan images. This study was supported by the ANR Program THEODULE.

References: [1] Zanda B. (2004) *EPSL, 224,* 1–17. [2] Sorby H. C. (1877) *Nature, 15,* 495–498. [3] Desch S. J. et al. (2012) *MAPS, 47,* 1139–1156. [4] Shu F. H. et al. (2001) *Astroph. J., 548,* 1029–1050. [5] Desch S. J. and Cuzzi J. N. (2000) *Icarus, 143,* 87–105. [6] Hood L. L. et al. (2009) *MAPS, 44,* 327–342. [7] Desch S. J. and Connolly H. C. Jr. (2002) *MAPS, 37,* 183–207. [8] Morris M. A. and Desch S. J. (2010) *Astroph. J., 722,* 1474–1494. [9] Lofgren G. E. (1996) in *Chondr. Protopl. Disk*, 187–196. [10] Hewins R. H. et al. (2005) *Chondr. Protopl. Disk, 341,* 286–317. [11] Asphaug E. et al. (2011) *LPSC XLII, Abstract #1647.* [12] Weinbruch S. and Müller W. F. (1995) *GCA, 59,* 3221–3230. [13] Cuvillier P. et al. (2014) *LPSC XLV, Abstract #1711.* [14] Humayun M. (2012) *MAPS, 47,* 1191–1208. [15] Chaumard N. et al. (2014) *LPSC XLV, Abstract #2448.* [16] Righter K. et al. (2005) *GCA, 69,* 3145–3158. [17] Connolly H. C. et al. (2001) *GCA, 65,* 4567–4588. [18] Zanda B. et al. (2002) *LPSC XXXIII, Abstract #1852*.